Carbohydrate Polymers 108 (2014) 169–175

Contents lists available at ScienceDirect

Carbohydrate Polymers

journal homepage: www.elsevier.com/locate/carbpol

Nano-titania-crosslinked chitosan composite as a superior sorbent for antimony (III) and (V)

Padala Abdul Nishad, Anupkumar Bhaskarapillai*, Sankaralingam Velmurugan

Water and Steam Chemistry Division, Bhabha Atomic Research Centre Facilities, Kalpakkam 603102, Tamilnadu, India

ARTICLE INFO

Article history:
Received 18 December 2013
Received in revised form 26 February 2014
Accepted 28 February 2014
Available online 12 March 2014

Keywords:
Chitosan
Nano-TiO_2
Antimony
Sorption
Nuclear Reactor

ABSTRACT

Removal of radioactive antimony, especially at low levels, is a difficult problem faced by nuclear power plants all over the world. Further, antimony is classified as a pollutant of priority importance by the United States and the European environmental protection agencies. Chitosan, a biopolymer well known for its sorption properties, can also serve as a stable matrix for inorganic sorbents such as titania on crosslinking. A robust high performing sorbent for antimony, in the form of stable beads, has been prepared using nano-TiO_2 and chitosan. Raman spectra of the beads confirmed the incorporation of nano-TiO_2 in the chitosan matrix. The sorbent exhibited complete sorption of antimony from aqueous solutions with antimony concentrations ranging from as low as 150 ppb to as high as 120 ppm. The sorption dependence on equilibrium pH has been investigated. The beads have been shown to be effective sorbent of antimony in both +3 and +5 oxidation states. The sorption properties of the beads were attributed to the TiO_2 component present in the beads, while the crosslinked chitosan provided strong matrix and influenced the formation of much needed stable spherical beads suitable for real life large scale applications. The beads exhibited high sorption efficiency in the column mode, and were found to be physically stable at a flow rate of one bed volume per minute.

1. Introduction

Antimony, a metalloid by nature, finds its use mainly in flame retardants and as a constituent in hard alloys. It also finds use as a structural material in special applications such as nuclear reactors. Antimony impregnated graphite seals are commonly used in the coolant pumps of nuclear reactors. Due to routine wear and tear, antimony is released into the coolant. Such released antimony may get activated to active species of antimony (^{122}Sb, ^{124}Sb) on passing through the core of the reactor and lead to increased levels of radiation field (Neeb, 1997). These active nuclides may also remain deposited over the surfaces of the core and coolant channels. During routine decontamination of the reactors, carried out to reduce the radiation field, radioactive nuclides deposited over coolant surfaces are removed using complexant solutions (Ocken, 1999). The removed nuclides are trapped over ion exchange resin beds. Such decontamination campaigns are generally effective in removing various radionuclides such as cobalt, caesium, etc. and bring down the radiation field effectively. However, during some of the decontamination campaigns, the radiation field at some surfaces were seen to have actually gone up. This was found to be due to lack of removal of antimony isotopes by the cation IX columns used, which subsequently deposited over out of core surfaces leading to increased radiation field on those surfaces (Velmurugan et al., 2011). A process that involves oxidation of the antimony using hydrogen peroxide to Sb(V) has been reported to be effective in bringing the antimony deposits into solution which is to be removed over anion resin bed. The commonly used cation exchange columns have been found to be unsuitable for its removal as the antimony was predominantly present as anionic species. On the other hand, anion resins have been found to be effective in their removal; they however have the limitation in terms of its use in alkaline pH due to competition from the excess hydroxyl ions at typically found very low concentrations of antimony. Thus, there clearly is a need for a sorbent for effective removal of antimony, present at low levels, in nuclear reactors. Our work has been initiated primarily to address this concern.

Apart from such a specific application, since antimony and its compounds have been classified as pollutants of priority importance by the United States Environmental Protection Agency (USEPA) and the European Environment Agency (maximum contaminant level of 6 μg/L in drinking water as set by USEPA), there is increased attention in antimony removal during general waste

* Corresponding author. Tel.: +91 44 27480097; fax: +91 44 27480097.
E-mail addresses: anup@igcar.gov.in (A. Bhaskarapillai), svelu@igcar.gov.in (S. Velmurugan).

http://dx.doi.org/10.1016/j.carbpol.2014.02.091
0144-8617/

water treatment procedures. Further, most sorbents that are effective in Sb removal will most likely be a good sorbent for arsenic removal as well, as both share similar complexation chemistry. The existence of antimony in two different oxidation states (+3 and +5); mostly in the form of ionic hydroxyl species like $[Sb(OH)_6]^-$, $Sb(OH)_{3(aq)}$, $[Sb(OH)_4]^+$, etc., depending upon the solution conditions (Filella, Belzile, & Chen, 2002; Krupka, 2002), makes its separation very challenging. Based on thermodynamic data, in aqueous aerated solutions, $Sb(OH)_6^-$ is known to be the predominant species above pH 2.7. Different methodologies such as ion exchange (Riveros, 2010), solvent extraction (Navarro, Simpson, & Alguacil, 1999), adsorption (Li, Dou, & Li, 2012), coagulation and filtration (Wu, He, Guo, & Zhou, 2010; Zhu, Wu, Pan, Guo, & Wen, 2011), and membrane separation (Saito et al., 2004) have been studied for treatment of various types of antimony containing effluents from different industries. Removal of Sb by sorption materials, mainly inorganic hydroxides and some biosorbents, was found to be most promising in terms of removal efficiency, ease of availability and applicability (Bakir, McLoughlin, Tofail, & Fitzgerald, 2009; Biswas, Inoue, Kawakita, Ohto, & Inoue, 2009; Watkins et al., 2006). Quantitative separation of nanogram levels of antimony from other metals such as manganese and iron was demonstrated using substituted cellulose as the sorbent material (Muzzarelli & Marcotrigiano, 1967). Metal oxide sorbents, TiO_2 in particular, have been found to be promising in removal of Sb (Mukhopadhyay & Lahiri, 2007) and As (Guan et al., 2012), which are otherwise difficult to remove using regular ion exchange resins. Mukhopadhyay and Lahiri (2007) reported batch sorption studies that demonstrated fast and irreversible sorption of radioactive antimony (^{125}Sb) by titania. The sorption mechanism involved with TiO_2 and As has been dealt with in detail in the literature (Han, Abdel-Wahab, & Batchelor, 2010; Pena, Meng, Korfiatis, & Jing, 2006).

Both chitosan and TiO_2 have been reported extensively as sorbent materials for metal ions and organic compounds (Muzzarelli, 2011; Muzzarelli & Tubertini, 1969; Padala, Bhaskarapillai, Velmurugan, & Narasimhan, 2011; Pavlík, Semelová, John, Černochová, & Šebesta, 2006). The former has been explored widely for developing sorbents for targeted nuclear related applications as well (Muzzarelli & Tubertini, 1972; Padala, Bhaskarapillai, Velmurugan, & Narasimhan, 2012), while the latter in particular has been reported to be an effective sorbent for arsenic (Guan et al., 2012) and for the photo catalytic removal of anionic species (Akpan & Hameed, 2009). TiO_2 in nano form has excellent sorption properties due to the enhanced surface area available for the sorbate. However, it has post treatment issues in removal of the sorbent, making it unviable for either a batch mode or column mode operation in large scale applications. Thus, in order to make use of the sorption efficiency of the nano-TiO_2, it is important to be able to prepare them in useable format, such as beads of regular size and shape. As it is difficult to prepare the oxide in bead formats, a logical approach would be to incorporate the TiO_2 into a matrix, such as chitosan, that can be prepared in such a format. Mechanical properties of the chitosan were reported to be improved by the addition of TiO_2 (Al-Sagheer & Merchant, 2011; Amin & Panhuis, 2012), which was attributed to the homogeneous distribution of the titania particles in the chitosan matrix by the interfacial interaction between the basic amine sites ($-NH_2$) in the biopolymer with the Lewis acidic sites present in the titania (Al-Sagheer & Merchant, 2011). Shchipunov (2012) has reviewed the potential applications of various such bionanocomposites.

Miller, Spaulding, and Zimmerman (2011) have prepared TiO_2 impregnated chitosan beads (TICB) and demonstrated the arsenic sorption efficiency of the beads. However, the use of TICB was reported to be limited by the solution pH. As the chitosan matrix in the beads was not crosslinked, the beads lacked stability in acidic media. It was found to disintegrate into solution at pH less than 4.0. This could be prevented by cross linking of the chitosan as it would make the beads insoluble and impart better chemical and mechanical stability. Such attempts have been made to obtain TiO_2 based materials with enhanced photocatalytic activity (Li, Su, & Tan, 2008; Su, Li, & Tan, 2006) and high organic decomposition efficiency (Zhang, Zhao, & Su, 2011). Herein we report the preparation of stable composite beads using nanoTiO_2 and crosslinked chitosan through a simple reproducible procedure and demonstrate the efficiency of the beads as sorbent material for antimony. We further show, through column studies, that the beads have high potential for use in large scale operations.

2. Experimental details

2.1. Materials and instruments

Chitosan, medium molecular weight (Brookfield viscosity 200–800 cP, 1 wt.% in 1% acetic acid, 25 °C), 75–85% deacetylated, and potassium hexahydroxo antimonate ($KSb(OH)_6$) were obtained from Sigma–Aldrich. Nano-titania (as TiO_2 powder containing 17–18% moisture; 10–15 nm size, special grade) was from Travancore Titanium Products Limited, Trivandrum, India. Epichlorohydrin, purchased from Loba Chemie, India, was of synthesis grade. All the other chemicals were of AR grade and were received from either HiMedia or SDFCL, India. Chemicals were used as supplied. All the sample solutions were prepared in ultra pure water (Sartorius Arium®611). Sb(V) and Sb(III) solutions were prepared using $KSb(OH)_6$ and potassium antimony (III) tartarate, respectively.

Raman spectra were recorded using a dispersive micro Raman Spectrometer (HR-800), Jobin Yvon, France. Argon ion laser, 514 or 785 nm, was focused using a 50× LD objective lens on sample surface with laser power of 0.5–1.0 mW. 1800 groves/mm grating was used with 15–30 s data acquisition time. Antimony concentrations were measured using ICP-AES (Ultima2 Horiba Jovin Yvon, France). Irradiation studies were done in a gamma chamber containing cobalt source with a dose rate of 5.852 kGy/h. Solution pH measurements were done using a glass electrode. Surface area (BET) measurements were done with nitrogen sorption (Thermoelectron, Sorptomatic 1990), while the pore size measurements were done using mercury porosimetry (ThermoFischer Scientific). Bead size measurements were done using an electronic Vernier scale (Mitutoyo digimatic calliper).

2.2. Synthesis of the nano-titania-crosslinked chitosan composite (TA-chitosan) beads

About 0.5 g of the chitosan was dissolved in 20 mL of 3% acetic acid (v/v) solution. To this solution, nano-titania (0.1 g) was added with stirring. The mixture was sonicated for 15 min followed by addition of the crosslinking agent epichlorohydrin (1 mL) with stirring. The resultant dispersion was taken in a 10 mL glass syringe and added as drops at a rate of 1 mL/min through a 22 gauge needle into a 0.25 M NaOH solution kept at room temperature (27 °C), under constant stirring (at 400 rpm), leading to formation of solid beads. Stirring was done with a magnetic stirrer plate and a pellet of dimensions 23.0 (L) × 7.8 mm (W). The entire solution was added through the same syringe and needle by refilling. The precipitated beads were left overnight at room temperature to remain in the solution without stirring. The beads were separated, washed with ultra pure water and dried overnight in an air oven at 50 °C. The dried beads were treated with 10 mL of 0.1 M HCl for 6 h in order to remove any un-reacted chitosan. The beads were further washed with ultra pure water to get neutral washings, and dried

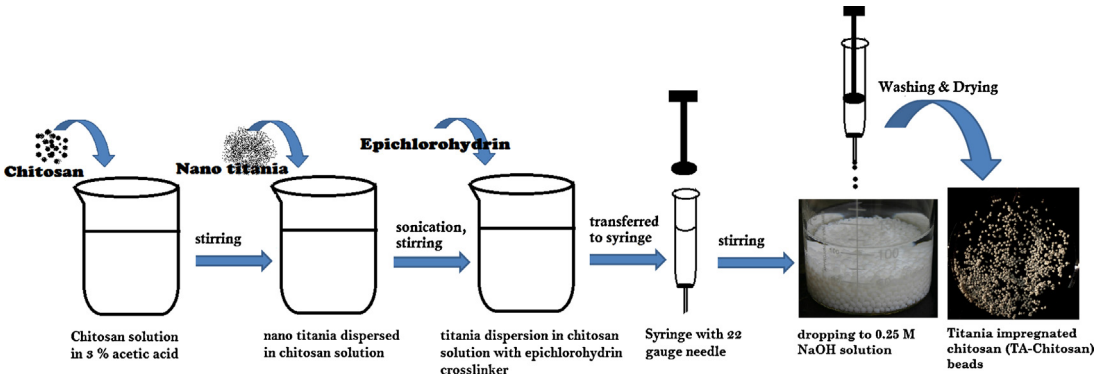

Fig. 1. Scheme for the synthesis of nano-titania-crosslinked chitosan composite (TA-chitosan) beads.

under vacuum. The purified dry beads thus obtained were used as the nano-titania-crosslinked chitosan composite (TA-chitosan) beads for the sorption studies.

2.3. Swelling studies

Around 400 mg of the TA-chitosan beads were swollen by adding it to a measuring cylinder containing 3 mL ultra pure water (swelling agent). The beads were then separated from the water and the surface water was removed by blotting with filter paper. The weight of the swollen beads was recorded. Swelling characteristics were expressed as Equilibrium swelling ratio (E_{SR}, Eq. (1)) and Equilibrium Water Content (E_{WC}, Eq. (2)) (Raj Singh, McCarron, Woolfson, & Donnelly, 2009).

$$E_{SR} = \frac{W_s - W_d}{W_d} \quad (1)$$

where, W_s and W_d are the swollen and dry weights of the TA-chitosan beads respectively.

$$E_{WC} = \frac{W_e - W_d}{W_e} \quad (2)$$

where W_e and W_d are the weight of the TA-chitosan beads in the swollen state at equilibrium and in the dry state respectively.

2.4. Sorption studies

Batch sorption studies were carried out by equilibrating a known amount of the sorbent with known volume of the antimony solution on a rotator. The amount of antimony sorbed (sorption capacity, q_t (μmol/g)), on equilibration for time t, was obtained as

$$q_t = \frac{(C_i - C_f)V}{W} \quad (3)$$

where, C_i and C_f are respectively the initial and final liquid phase concentrations (μmol/L) of the antimony solutions; V is the volume of the solution in litre, and W is the weight of the sorbent in gram.

3. Results and discussions

3.1. Synthesis and characterisation of the TA-chitosan beads

3.1.1. Synthesis

The synthesis scheme used for preparation of the TA-chitosan beads is shown in Fig. 1. The mixture containing the chitosan solution, TiO_2 and crosslinker on dropping into alkaline solution formed stable beads. The bead sizes could be controlled based on the gauge of the needle used for dropping the mixture. As the process involved is simple and easy to scale up; proper control over the bead size and properties can be achieved with minimal efforts. The bead size of the synthesised beads was found to be 0.79 mm (± 0.09 mm). The bead size was obtained as mean of bead size of 16 randomly chosen beads.

3.1.2. Characterisation of nano-TiO_2 and the TA-chitosan beads

Raman spectrum of the nano-TiO_2 (shown in SD), containing 17–18% moisture, used for the synthesis of the beads, showed it to be of anatase phase. On oven drying at 150 °C for 1 h, the Raman peaks corresponding to water disappeared indicating the presence of water in the nano-TiO_2 as moisture content. Thermo gravimetric analysis also showed the weight loss corresponding to the water loss (data not shown). The specific surface area of the nano-TiO_2 was found to be 146.1 m^2/g. The lattice parameter calculated from the XRD spectrum of the nano-TiO_2 (spectrum in SD) used for the synthesis matched with the reported values for anatase (Legrand & Delville, 1953) indicating the presence of single phase (anatase) in the nano-TiO_2 used for preparation of the beads.

The Raman spectra of the starting materials namely, chitosan, nano-TiO_2 and the TA-chitosan beads synthesised are shown in Fig. 2. The Raman spectra of the TA-chitosan beads showed TiO_2 peaks (148 (not shown in the spectrum of the TA-chitosan beads), 394, 515 and 638 cm^{-1}) and the peaks due to chitosan (899, 1110 and 1378 cm^{-1}), indicating their respective presence.

The surface area measurements (nitrogen sorption) have shown the specific surface area of the TA-chitosan beads to be 3.9 m^2/g. The low surface area of the beads can be explained by the fact that the major component of the beads was chitosan, whose

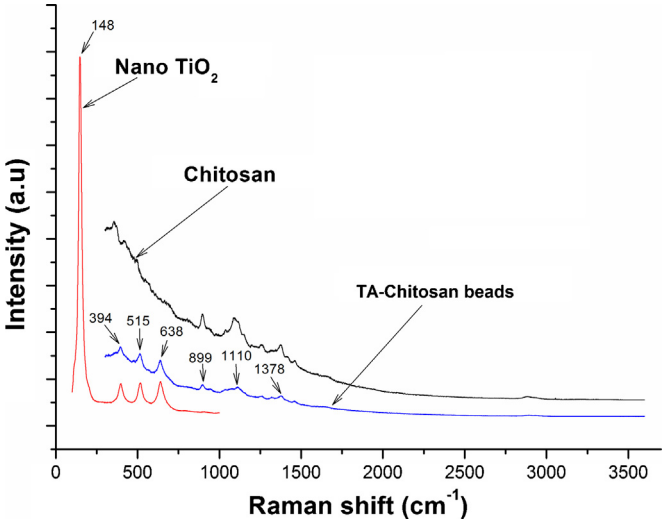

Fig. 2. Raman spectra of nano-TiO_2, chitosan, and nano-titania-crosslinked chitosan composite (TA-chitosan) beads.

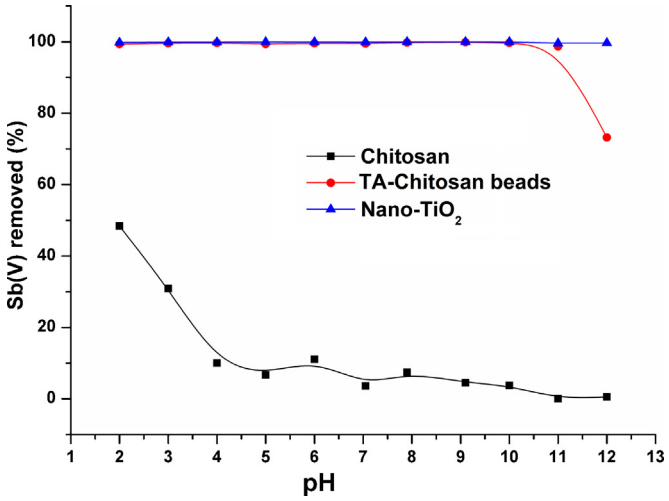

Fig. 3. Effect of solution pH (initial) on Sb(V) sorption.

surface area was found to be 5.8 m^2/g. Porosity measurements (mercury porosimetry) have shown that the TA-chitosan beads were mesoporous (median pore diameter: 6.95 nm at 14.6 mm^3/g) with narrow pore size distribution. The accessible porosity of the beads was found to be 4.31%.

3.2. Swelling characteristics of the TA-chitosan beads

Swelling behaviour of the TA-chitosan beads was measured by overnight swelling of the dry beads in ultra pure water at room temperature (solution temperature: 27 °C). TA-chitosan beads showed an almost instantaneous swelling; nearly 90% of the volume expansion was achieved within 5 min. The wet volume of the swollen TA-chitosan beads was about 2.0 mL. Equilibrium swelling ratio (Eq. (1)) and equilibrium water content (Eq. (2)) were calculated to be 200.1% and 66.6% respectively. Similar swelling parameters have been reported for glutaraldehyde and glyoxal crosslinked chitosan microspheres (Gupta & Jabrail, 2006).

3.3. Evaluation of the sorption properties

3.3.1. Batch sorption of Sb(V) by the TA-chitosan beads, chitosan and nano-TiO_2: effect of pH

Antimony (V) sorption (as $Sb(OH)_6^-$) efficiency of the composite TA-chitosan beads and the constituents of the beads namely, chitosan and nano-TiO_2 was studied in batch mode. A 1 mM solution (1 mL) of Sb(V) (made from $KSb(OH)_6$) was equilibrated with 10 mg of the sorbent for evaluating its sorption properties. Fig. 3 shows the effect of initial pH of the solution on sorption. The initial solution pH was adjusted to the desired value using dilute HCl or NaOH solutions. Chitosan sorbed Sb(V) only at acidic conditions. This is expected as the amino groups of the chitosan are protonated under acidic conditions (Navarro, Guzmán, Saucedo, Revilla, & Guibal, 2003) and the resultant quaternary amine groups bind the anionic $Sb(OH)_6^-$ species. Unlike chitosan, nano-TiO_2 and TA-chitosan beads showed high pick up of Sb(V) over wide range of pH conditions (Fig. 3). It can be seen that the sorption properties of the TA-chitosan beads are almost identical with that of nanoTiO_2. Thus, the removal of Sb(V) by the TA-chitosan beads is mainly effected by the nano-titania rather than the chitosan. Chitosan serves as a stable matrix that holds the nano-TiO_2 responsible for the antimony sorption. Crosslinking of the chitosan has made the composite beads insoluble in acidic solutions, thus giving the beads stability under wide pH conditions. The pH values shown in Fig. 3 correspond to the initial solution pH. During sorption, it

Table 1
Effect of solution pH on sorption equilibrium.

Sorbent	Sb(V) initial concentration (ppb)	Solution pH		Sb(V) sorbed (%)
		Initial	Equilibrium	
Nano-TiO_2	153.5	10.0	4.9	100
TA-chitosan beads	153.5	10.0	4.8	95.8
TA-chitosan beads	154.5	10.8	10.7	Nil

was observed that the pH of the solution changed significantly on equilibration. The equilibrium pH values attained during the sorption studies with low (ppb level) solution concentrations of Sb(V) (solution to sorbent ratio: 50 mL to 10 mg) are shown in Table 1. The solution pH was seen to change drastically from the initial value of 10.0–4.9 on equilibration, accompanied with complete removal of antimony. The results in the table clearly indicate the strong dependence of the sorption on equilibrium pH.

This dependence was further evaluated in detail by maintaining constant solution pH (dilute HCl/NaOH) till the sorption was complete. These sorption studies were done by equilibrating 30 mg TA-chitosan beads, with 6 mL of 1 mM Sb(V) solution of different initial pH values. For each experiment, the addition of dilute HCl/NaOH was continued till there was no more sorption and any associated measurable change in the solution pH. The solution pH increased slowly on addition of the sorbent to the solution having initial pH of 2.0, while in all other cases there was a decrease in solution pH during sorption. These observations can be explained based on the pH dependant nature of charge density present on the TiO_2 surface exposed to water. As shown in Eq. (4), which depicts the pH dependent surface charge on TiO_2, at low pH, the surface is predominantly positively charged, leading to sorption of hydroxyl and other anionic species. The hydroxyl ion sorption leads to reduction in the solution pH when the sorbent is equilibrated with alkaline solution.

$$\mathrm{Ti(IV)-OH_2^+ \rightleftharpoons Ti(IV)-OH \rightleftharpoons Ti(IV)-O^-} \quad \text{(Increasing pH)} \tag{4}$$

During the synthesis, as the beads have been finally treated with dilute acid, majority of the surface is expected to be positively charged. When exposed to antimony solution of very low pH of 2.0, there is increased protonation of sites that were not protonated (or de-protonated during the final aqueous wash) during the synthesis, leading to increase in the solution pH. The decrease in solution pH on exposure of the beads to pH beyond 2.0 is attributable to the sorption of hydroxyl ions by the positive sites on the bead.

As the pH increases, the surface tends more towards negative charge thereby leading to reduced pick up of $Sb(OH)_6$ anions, as reflected by the drastic reduction in Sb(V) sorption at equilibrium pH beyond 5.0 (Fig. 4). It is to be noted that when antimony solution of initial pH of 10.0 was equilibrated with the beads, there was complete sorption and the equilibrium pH was close to 5.0. This observation indicates that the very high capacity of the beads makes it possible for the sorbent to sorb the anionic species of Sb(V) even from such highly alkaline solution. Such a high capacity is attributable to the nano form of the TiO_2 and the hydrophilic nature of the composite beads that gives easy access to the anionic species.

In order to investigate the contribution towards change in pH during sorption by the individual components of the composite beads, 8 mL of the 1 mM Sb(V) solution was equilibrated with 40, 7 and 34 mg of the TA-chitosan beads, nano-titania and chitosan respectively. The amount of titania and chitosan was calculated to correlate with their respective amounts present in the TA-chitosan beads. The change in pH and the sorption capacities of the sorbents

Table 2
Change in pH associated with Sb(V) sorption (from 1 mM solution) by the sorbents.

Sorbent	Amount of Sb(V) sorbed			pH_{eq}	$\Delta pH(pH_{eq} - pH_{in})$[a]
	μmol/g of sorbent	μmol/g of nano-TiO_2 present in the sorbent	As % of initial amount		
Nano-TiO_2	799.1	799.1	69.7	3.33	−1.99
TA-chitosan beads	202.5	1357.4	98.6	3.67	−1.65
Chitosan	4.2	–	2.9	6.96	+1.64

[a] pH_{eq} – equilibrium pH; pH_{in} – initial pH.

(Table 2) indicate that the sorption is essentially by the TiO_2 component rather than the chitosan matrix. The pH increase associated with equilibration of chitosan is due to proton abstraction by the amino groups present, as the initial pH was less than the pK_a (~6.5) of the NH_2 groups of the chitosan (Navarro et al., 2003). Its contribution is reflected in the reduced change in pH with the beads as compared to that of the nano-TiO_2. The third column in Table 2 shows the capacity value calculated for the amount of TiO_2 present per unit mass of the TA-chitosan beads. The capacity values thus obtained show that the sorption by the TiO_2 component present in the TA-chitosan beads is 1.5 times more than the sorption capacity of the neat nano-TiO_2. Thus it is evident that nano-titania in combination with chitosan in the form of composite beads is a much better sorbent for Sb(V) as compared to neat nano-titania.

3.3.2. Kinetics of Sb(V) sorption/desorption by TA-chitosan beads

Sorption studies were carried out with 40 mg of the sorbent with 8 mL of 1.0 mM Sb(V) solution, with initial pH of 5.2, in batch mode. Samples were taken at regular intervals and analysed for antimony concentration using ICP-AES. TA-chitosan beads showed fast uptake of antimony with almost complete removal of antimony from the solution within 30 min (data in SD).

Complete desorption of the sorbed Sb(V) from the sorbent could not be achieved, indicating a strong binding by the sorbent. Maximum desorption attained was about 30–40% using 0.25 M NaOH by prolonged equilibration (about 70 h). Apart from electrostatic attraction of the anionic species by the surface charges on the TiO_2, there is a possibility of strongly bound complex formation with the surface titanium dioxide sites (Gonçalves, Gushikem, & de Castro, 1999). The low rate of desorption indicates the possibility of such a strong binding of antimony by the sorbent.

3.3.3. Batch sorption of Sb(III) by TA-chitosan beads

Apart from +5 oxidation state, +3 is another common stable oxidation state for antimony in aqueous solutions (vide supra). During nuclear reactor decontaminations, antimony is expected to be predominantly present as Sb(III) when the process is carried out under reducing conditions. Batch sorption studies were carried out to quantify the sorption of antimony in its Sb(III) form (from potassium antimony(III) tartarate solution) by the sorbents. Table 3 shows the effect of solution pH on the Sb(III) sorption and the extent of sorption induced change in the solution pH. There was Sb(III) hydrolysis leading to its precipitation at pH conditions beyond neutral pH. As with Sb(V) sorption, there was significant change in the pH during sorption as evidenced by the equilibrium pH values. Complete sorption of Sb(III) was seen even at low solution concentrations (Fig. 5a). Fig. 5b shows that the saturation capacity of 2.14 mmol/g was reached at initial concentration above 2400 ppm. Thus the synthesised beads are effective sorbents for both the forms of antimony from aqueous solutions.

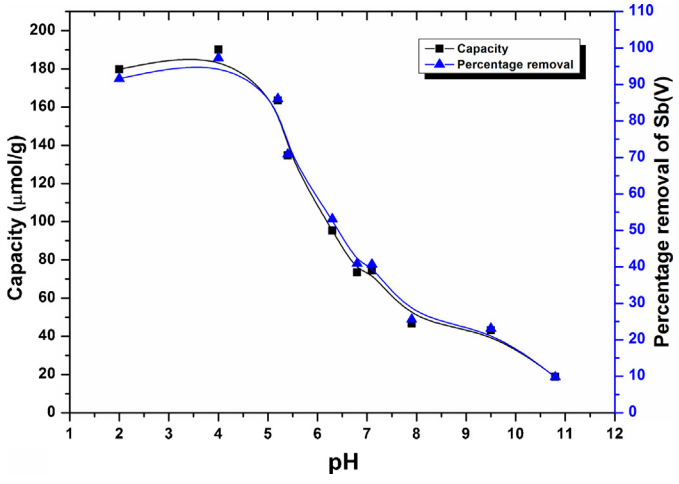

Fig. 4. Sb(V) sorption when solution pH is (forcefully) kept constant.

3.4. Suitability of TA-chitosan beads for column mode of operation in continuous mode

The utility of a resin is enhanced if it has flow properties and sorption kinetics suitable for column mode of operation. Therefore, suitability of TA-chitosan beads for use as column material was evaluated. About 250 mg (dry weight) of the TA-chitosan beads was fully wet in ultra pure water and then transferred to a glass chromatography column (provided with a Teflon stopper) of diameter of about 0.45 cm and 15 cm length. A small amount of glass wool was packed at the end of the column over which, the sorbent was filled to a length of 10 cm. The sorbent was filled by pouring the beads suspended in water into the column. Compact channel free filling was ensured by slow filling under constant flow and continuous tapping of the column while filling. The bed volume was 2 mL. About 2.5 L of Sb(V) solution of concentrations 1 ppm and 10 ppm were passed through the column in once through mode at a constant flow rate of 2 mL/min (one bed volume per minute). The outlet was collected for known time intervals and sampled for metal ion estimations (A flow chart depicting the column experiment is included in the supplementary data). The column was found to be very stable and the flow rate could be maintained constant throughout during the operation without any sign of back pressure or reduction in the flow rate. Thus the beads have flow properties suitable for column mode of operation. The Sb(V) concentrations in the outlet of the column were measured with time. The amount of antimony removed by the column filled with TA-chitosan beads is plotted against time in Fig. 6. There was a smooth decrease in sorption with time. The small humps around 480 and 960 min were because of the stagnant solution inside the column during its stoppage and restarting on the consecutive days. The maximum sorption capacity obtained was 508 μmol of antimony per gram of the TA-chitosan sorbent on passing 2.5 L of 10 ppm Sb(V) solution.

3.5. Investigation on the suitability of TA-chitosan beads for antimony removal during nuclear reactor decontamination

For the beads to be applicable during nuclear reactor decontamination, the beads (a) should be suitable as a column material (b) should have radiation stability and (c) remove antimony from typical decontamination formulation consisting of mixture

Table 3
Solution pH dependence of Sb(III) sorption by the sorbents.[a]

Sorbent	pH (initial): 3.06			pH (initial): 6.90		
	Sorption capacity for Sb(III) (μmol/g)	Sb(III) sorbed (%)	pH_{eq}	Sorption capacity for Sb(III) (μmol/g)	Sb(III) sorbed (%)	pH_{eq}
Nano-TiO_2	187.7	100	2.42	173.2	100	2.67
Chitosan	93.8	52.2	6.27	0	0	7.50
TA-chitosan beads	181.5	97.1	3.50	170.3	95.5	4.23

[a] 25 mg sorbent equilibrated with 5 mL of 1 mM Sb(III) solution for 24 h; pH_{eq} – equilibrium pH.

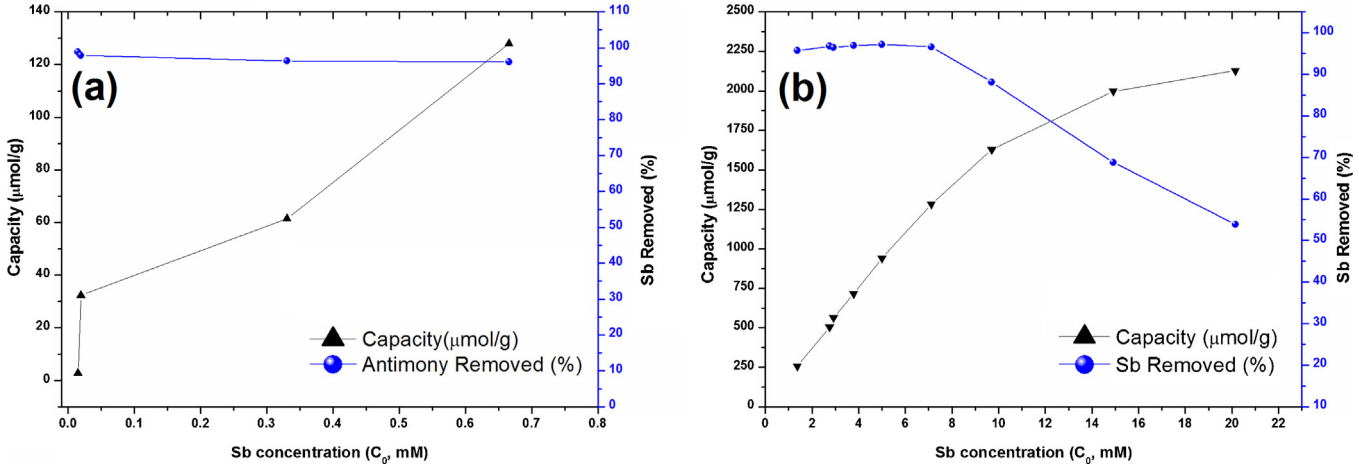

Fig. 5. Effect of initial concentration ($pH_{initial}$ = 4.5) on Sb(III) sorption by nano-titania-crosslinked chitosan composite (TA-chitosan) beads (a) lower concentration range and (b) higher concentration range.

of complexing agents. The suitability of the beads under column conditions has been established (vide supra). Batch sorption studies have been carried out to examine the other two factors. The radiation stability was investigated by irradiating a vial containing deaerated 1 mM Sb(V) solution (10 mL) and 50 mg TA-chitosan beads to different doses. The irradiated solutions were left outside to complete the equilibration time of 7 h and analysed for antimony concentration and TOC. The sorption results (Table 4) showed that there was no negative effect on the sorption on irradiation. The marginal increase in capacity with increased dose is attributable to the associated increase in the solution temperature due to irradiation. Measurement of TOC in the irradiated solutions indicated that there was no significant release of organics (due to decomposition) on irradiation.

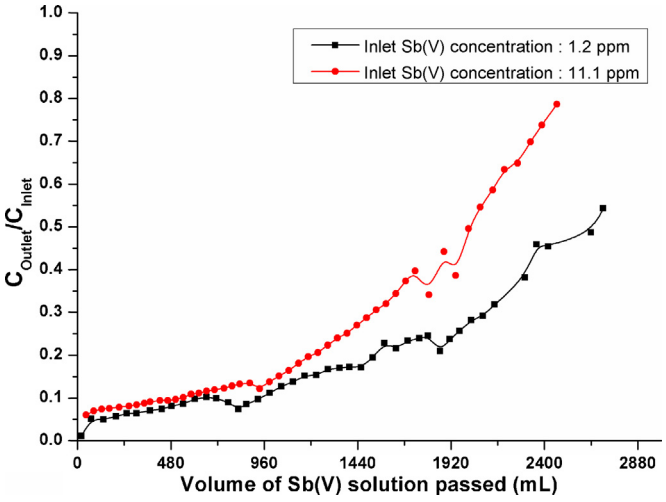

Fig. 6. Removal Sb(V) from the solution by a column filled with the nano-titania-crosslinked chitosan composite (TA-chitosan) beads (C_{outlet} = Sb(V) concentration at the column outlet; C_{inlet} = Sb(V) concentration at the column inlet; flow rate: 2 mL/min).

Table 4
Effect of irradiation on antimony sorption (from 1 mM solution) by TA-chitosan beads ($pH_{initial}$ = 5.5; pH_{eqbm} = 3.5).

Dose (kGy)	Sorption Capacity for Sb(V) (μmol/g)	Sb(V) sorbed (%)
0	154.0	76.4
2	166.7	80.3
20	185.8	90.3

The sorption of antimony from typical decontamination (NAC) formulation (Rufus, Velmurugan, Sathyaseelan, & Narasimhan, 2004) containing Nitrilotriacetic acid (1.37 mM or 262 ppm), Ascorbic acid and Citric acid (300 ppm each) was investigated by batch sorption. The results obtained (Table 5), on equilibration of the TA-chitosan beads (10 mg) with NAC solution (10 mL) containing antimony (Sb(III)/Sb(V)) for 24 h, show that the beads were able to sorb 80% of the antimony present from the NAC solution containing 100 ppb of Sb(III). The sorption, however, was reduced in the case of Sb(V). The results indicate that the beads will be more useful when the decontamination is carried out under reducing conditions, which generally is the case (Rufus et al., 2004), wherein antimony is present in +3 form rather than in +5 (Krupka, 2002).

Table 5
Sorption of antimony by the TA-chitosan beads from complexing (NAC) medium.

Metal ion solution	Sorption capacity (μmol/g)	Antimony removed (%)
150 ppb Sb(V) solution in NAC medium	0.411	36.8
150 ppb Sb(III) solution in NAC medium	1.013	81.8
150 ppb each Sb(III) and Sb(V) solution in NAC medium	1.333	52.1

4. Conclusions

Chitosan-nano-titania (TA-chitosan) composite sorbent was synthesised as beads and studied for its antimony sorption properties. The beads were shown to be effective sorbent for antimony in both +3 and +5 forms. Preparation of the sorbent in the form of beads makes it more suitable form for the envisaged large scale application. TA-chitosan beads showed sorption characteristics similar to its parent compound nano-titania in terms of uptake capacity and equilibrium pH of sorption, while the format was more suitable for column application unlike the parent nano-TiO_2. The procedure adopted for making the TA-chitosan beads has been shown to yield better and stable beads that can be utilised even under acidic conditions. Further, the beads were shown to be stable and suitable for column mode operation, with reasonably high dynamic capacity of 500 μmol/g. This is the first study that shows promise in using nano-TiO_2 based sorbent for removal of antimony in column mode operation and further studies are in progress for optimisation of the bead characteristics for various applications.

Acknowledgements

The authors thank Dr. K.V.G. Kutty and Mr. Madhavan, MCD, IGCAR Kalpakkam for the nano-TiO_2 sample and its TGA and XRD spectra; Dr. P. Chandramohan, WSCD, BARC (F) Kalpakkam for the Raman spectra and nitrogen sorption measurement, and Dr R. Venkata Krishnan, Fuel Chemistry Division, IGCAR, Kalpakkam for mercury porosimetry.

Appendix A. Supplementary data

Supplementary data associated with this article can be found, in the online version, at http://dx.doi.org/10.1016/j.carbpol.2014.02.091.

References

Akpan, U. G., & Hameed, B. H. (2009). Parameters affecting the photocatalytic degradation of dyes using TiO_2-based photocatalysts: A review. *Journal of Hazardous Materials*, *170*(2–3), 520–529.

Al-Sagheer, F. A., & Merchant, S. (2011). Visco-elastic properties of chitosan–titania nano-composites. *Carbohydrate Polymers*, *85*(2), 356–362.

Amin, K. A. M., & Panhuis, M. i. h. (2012). Reinforced materials based on chitosan, TiO_2 and Ag Composites. *Polymers*, *4*(4), 590–599.

Bakir, A., McLoughlin, P., Tofail, S. A. M., & Fitzgerald, E. (2009). Competitive sorption of antimony with zinc, nickel, and aluminum in a seaweed based fixed-bed sorption column. *CLEAN – Soil, Air, Water*, *37*(9), 712–719.

Biswas, B. K., Inoue, J.-I., Kawakita, H., Ohto, K., & Inoue, K. (2009). Effective removal and recovery of antimony using metal-loaded saponified orange waste. *Journal of Hazardous Materials*, *172*(2–3), 721–728.

Filella, M., Belzile, N., & Chen, Y.-W. (2002). Antimony in the environment: A review focused on natural waters: II. Relevant solution chemistry. *Earth-Science Reviews*, *59*(1–4), 265–285.

Gonçalves, J. E., Gushikem, Y., & de Castro, S. C. (1999). Preparation and properties of antimony (V) oxide adsorbed on silica–titania mixed oxide. *Journal of Non-Crystalline Solids*, *260*(1–2), 125–131.

Guan, X., Du, J., Meng, X., Sun, Y., Sun, B., & Hu, Q. (2012). Application of titanium dioxide in arsenic removal from water: A review. *Journal of Hazardous Materials*, *215–216*, 1–16.

Gupta, K. C., & Jabrail, F. H. (2006). Glutaraldehyde and glyoxal cross-linked chitosan microspheres for controlled delivery of centchroman. *Carbohydrate Research*, *341*(6), 744–756.

Han, D. S., Abdel-Wahab, A., & Batchelor, B. (2010). Surface complexation modeling of arsenic (III) and arsenic (V) adsorption onto nanoporous titania adsorbents (NTAs). *Journal of Colloid and Interface Science*, *348*(2), 591–599.

Krupka, K. M., & Serne, R. J. (2002).. *Geochemical Factors Affecting the Behavior of Antimony, Cobalt, Europium, Technetium, and Uranium in Vadose Sediments* (Vol. PNNL-14126) Richland, WA: Pacific Northwest National Laboratory.

Legrand, C., & Delville, J. (1953). Sur les parametres cristallins du rutile et de l'anatase. *Comptes rendus hebdomadaires des seances de l'Academie des sciences*, *236*, 944.

Li, Q., Su, H., & Tan, T. (2008). Synthesis of ion-imprinted chitosan–TiO_2 adsorbent and its multi-functional performances. *Biochemical Engineering Journal*, *38*(2), 212–218.

Li, X., Dou, X., & Li, J. (2012). Antimony (V) removal from water by iron-zirconium bimetal oxide: Performance and mechanism. *Journal of Environmental Sciences*, *24*(7), 1197–1203.

Miller, S. M., Spaulding, M. L., & Zimmerman, J. B. (2011). Optimization of capacity and kinetics for a novel bio-based arsenic sorbent, TiO_2-impregnated chitosan bead. *Water Research*, *45*(17), 5745–5754.

Mukhopadhyay, B., & Lahiri, S. (2007). Adsorption of 125Sb on alumina and titania surfaces. *Journal of Radioanalytical and Nuclear Chemistry*, *273*(2), 423–426.

Muzzarelli, R. A. A. (2011). Potential of chitin/chitosan-bearing materials for uranium recovery: An interdisciplinary review. *Carbohydrate Polymers*, *84*(1), 54–63.

Muzzarelli, R. A. A., & Marcotrigiano, G. (1967). Applications of radioisotopes in chromatography on substituted celluloses: The separation of antimony from manganese, iron and other metals. *Talanta*, *14*, 489–494.

Muzzarelli, R. A. A., & Tubertini, O. (1969). Chitin and chitosan as chromatographic adsorbents and supports for collection of trace metals from aqueous and organic solutions and sea water. *Talanta*, *16*, 1571–1579.

Muzzarelli, R. A. A., & Tubertini, O. (1972). Radiation resistance of chitin and chitosan applied in the chromatography of radioactive solutions. *Journal of Radioanalytical and Nuclear Chemistry*, *12*(1), 431–440.

Navarro, P., Simpson, J., & Alguacil, F. J. (1999). Removal of antimony (III) from copper in sulphuric acid solutions by solvent extraction with LIX 1104SM. *Hydrometallurgy*, *53*(2), 121–131.

Navarro, R., Guzmán, J., Saucedo, I., Revilla, J., & Guibal, E. (2003). Recovery of metal ions by chitosan: Sorption mechanisms and influence of metal speciation. *Macromolecular Bioscience*, *3*(10), 552–561.

Neeb, K.-H. (1997). *The radiochemistry of nuclear power plants with light water reactors*. Berlin: Walter De Gruyter.

Ocken, H. (1999, July). *Decontamination handbook* (Vol. TR-112352) Palo Alto, CA: EPRI.

Padala, A. N., Bhaskarapillai, A., Velmurugan, S., & Narasimhan, S. V. (2011). Sorption behaviour of Co(II) and Cu(II) on chitosan in presence of nitrilotriacetic acid. *Journal of Hazardous Materials*, *191*(1–3), 110–117.

Padala, A. N., Bhaskarapillai, A., Velmurugan, S., & Narasimhan, S. V. (2012). Cobalt (II) imprinted chitosan for selective removal of cobalt during nuclear reactor decontamination. *Carbohydrate Polymers*, *87*, 2690–2696.

Pavlík, A., Semelová, M., John, J., Černochová, K., & Šebesta, F. (2006). Treatment of spent NTA-based decontamination solutions. *Czechoslovak Journal of Physics*, *56*(4), D673–D680.

Pena, M., Meng, X., Korfiatis, G. P., & Jing, C. (2006). Adsorption mechanism of arsenic on nanocrystalline titanium dioxide. *Environmental Science & Technology*, *40*(4), 1257–1262.

Raj Singh, T. R., McCarron, P. A., Woolfson, A. D., & Donnelly, R. F. (2009). Investigation of swelling and network parameters of poly(ethylene glycol)-crosslinked poly(methyl vinyl ether-co-maleic acid) hydrogels. *European Polymer Journal*, *45*(4), 1239–1249.

Riveros, P. A. (2010). The removal of antimony from copper electrolytes using amino-phosphonic resins: Improving the elution of pentavalent antimony. *Hydrometallurgy*, *105*(1–2), 110–114.

Rufus, A. L., Velmurugan, S., Sathyaseelan, V. S., & Narasimhan, S. V. (2004). Comparative study of nitrilo triacetic acid (NTA) and EDTA as formulation constituents for the chemical decontamination of primary coolant systems of nuclear power plants. *Progress in Nuclear Energy*, *44*(1), 13–31.

Saito, T., Tsuneda, S., Hirata, A., Nishiyama, S. Y., Saito, K., Saito, K., et al. (2004). Removal of antimony (III) using polyol-ligand-containing porous hollow-fiber membranes. *Separation Science and Technology*, *39*(13), 3011–3022.

Shchipunov, Y. (2012). Bionanocomposites: Green sustainable materials for the near future. *Pure and Applied Chemistry*, *84*(12), 2579–2607.

Su, H., Li, Q., & Tan, T. (2006). Double-functional characteristics of a surface molecular imprinted adsorbent with immobilization of nano-TiO_2. *Journal of Chemical Technology & Biotechnology*, *81*(11), 1797–1802.

Velmurugan, S., Rufus, A. L., Sathyaseelan, V. S., Mittal, V. K., Veena, S., & Narasimhan, S. V. (2011). Experience with dilute chemical decontamination in Indian pressurized heavy water reactors. *Energy Procedia*, *7*, 645–649.

Watkins, R., Weiss, D., Dubbin, W., Peel, K., Coles, B., & Arnold, T. (2006). Investigations into the kinetics and thermodynamics of Sb(III) adsorption on goethite (α-FeOOH). *Journal of Colloid and Interface Science*, *303*(2), 639–646.

Wu, Z., He, M., Guo, X., & Zhou, R. (2010). Removal of antimony (III) and antimony (V) from drinking water by ferric chloride coagulation: Competing ion effect and the mechanism analysis. *Separation and Purification Technology*, *76*(2), 184–190.

Zhang, X., Zhao, X., & Su, H. (2011). Degradation characteristic of TiO_2–chitosan adsorbent on Rhodamine B and purification of industrial wastewater. *Korean Journal of Chemical Engineering*, *28*(5), 1241–1246.

Zhu, J., Wu, F., Pan, X., Guo, J., & Wen, D. (2011). Removal of antimony from antimony mine flotation wastewater by electrocoagulation with aluminum electrodes. *Journal of Environmental Sciences*, *23*(7), 1066–1071.